IEEE Access
Multidisciplinary | Rapid Review | Open Access Journal

Received 11 January 2024, accepted 26 January 2024, date of publication 1 February 2024, date of current version 8 February 2024.

Digital Object Identifier 10.1109/ACCESS.2024.3361312

RESEARCH ARTICLE

Prospective LCA of Next-Generation Cells for Electric Vehicle Applications

ANTONELLA ACCARDO[1], AMBROGIO GAROFALO[1], GIOVANNI DOTELLI[2], AND EZIO SPESSA[1]

[1]Dipartimento Energia "Galileo Ferraris", CARS@PoliTO, Politecnico di Torino, 10129 Turin, Italy
[2]Dipartimento di Chimica, Materiali e Ingegneria Chimica "Giulio Natta", Politecnico di Milano, 20133 Milan, Italy

Corresponding author: Antonella Accardo (antonella.accardo@polito.it)

This work was supported by the Interdepartmental Center for Automotive Research and Sustainable Mobility (CARS), Politecnico di Torino.

ABSTRACT Several next-generation cells are now being researched to overcome the performance and sustainability limitations of the current Li-ion cells. The aim of this article is to assess the environmental impacts of the following next-generation cells chosen for their potential to meet the performance and safety requirements for future electric vehicle applications: Silicon-Polyacrylonitrile (SiCPAN), Silicon NanoWires (SiNWs), All-Solid-State (ASS) and Lithium-Sulphur (Li-S). Because the selected cells are emerging technologies, solely produced at the laboratory scale, a novel cradle-to-gate Prospective Life Cycle Assessment (P-LCA) was performed to ensure a fair comparison with the current Li-ion cell. The life cycle inventories of the selected cells were built by scaling up all the laboratory scale processes and activity data to industrial scale. The methodology is compliant with the most used frameworks for conventional LCAs, namely ISO 14040:2006 and ISO 14044:2018, and state-of-the-art guidelines for P-LCAs. The results showed that the Li-S cell has lower impact with respect to the current Li-ion cell in four out of the six most relevant impact categories, among which use of mineral and metal resources. The SiNWs cell revealed the greatest impact in almost all the impact categories. Lastly, a what-if analysis conducted on the silver content revealed that the ASS cell produced without silver would be the least impactful cell among the next-generation cells considered in this study.

INDEX TERMS Automotive, electric vehicles, energy storage systems, LCA, life cycle assessment, Li-ion batteries.

I. INTRODUCTION

A. CONTEXT

Annual global battery demand is expected to reach 1000 GWh by 2025 and 2600 GWh by 2030, with Europe alone creating 3–4 million jobs [1]. Li-ion batteries are currently a widely used and mature technology for powering Electric Vehicles (EVs) and a variety of other applications. However, the increasingly stringent requirements for EVs, among which are increased specific capacity and safety, are driving research into new battery technologies to overcome the limits of current Li-ion cells. According to the European Commission's Strategic Research Agenda for Batteries, it is critical to assess the novel cells of the so-called generation 3, 4, and 5 in order to have new, competitive European battery technologies available on the market by 2025 [1], [2].

From an environmental perspective, a novel Life Cycle Assessment (LCA) approach is emerging aimed at determining the environmental impacts of novel technologies [3]. In fact, according to [4], [5], [6], [7], and [8] a Prospective Life Cycle Assessment (P-LCA) or Ex-ante LCA should be performed. While conventional LCA is a well-known and valid tool for assessing the environmental sustainability of steady-state (i.e., mature, and commercialized) technologies, contrarily, for assessing emerging technologies where scaling effects must be included, a P-LCA is needed to ensure comparability between next-generation and current Li-ion batteries.

The associate editor coordinating the review of this manuscript and approving it for publication was Vitor Monteiro.

B. FUNDAMENTALS OF NEXT-GENERATION CELLS

While the current Li-ion cell mainly consists of a $LiNi_xMn_yCo_{1-x-y}O_2$ (NMC) cathode, a liquid electrolyte, and a graphite anode, next generation cells differ in one or more of these cell components.

In the so-called generation 3 cells, the graphite anode is substituted by a silicon-graphite anode. The wide interest in introducing silicon content into typical graphite anodes is due to the higher specific capacity of silicon (4200 mAh/g) compared to that of graphite (372 mAh/g) [9]. Nevertheless, silicon suffers from drastic volume change (up to 400%) during the charging and discharging process, which is the main barrier to its use in anodes [10]. A well-studied approach to reduce the above-mentioned issue consists of submitting the bulk silicon particles to dedicated chemical processes (e.g., metal deposition, chemical and metal-assisted chemical etching) to get multi-dimensional nanostructured silicon so that the final morphology is composed of Silicon NanoWires (SiNWs) [9], [11], [12]. An alternative process consists of encapsulating micro-silicon particles in a resilient, conductive coating of polyacrylonitrile (PAN) matrix so that the pulverization of the large silicon particles is reduced [13].

Generation 4 cells include the batteries with solid electrolytes, called Solid-State Batteries (SSBs), which are categorized into three types: sulfide-, oxide-, and, more recently, polymer-type. Because the solid electrolyte facilitates the coupling with a lithium metal anode, which as a specific capacity of 3860 mAh/g [10], SSBs nearly double the energy density of the best-performing Li-ion chemistry, resulting in a smaller and lighter battery pack [14]. Moreover, the absence of flammable liquid electrolytes in SSBs ensures increased safety [14]. Nevertheless, these batteries must overcome two major hurdles: a proper lithium deposition process at the anode and ionic conductivity of solid electrolytes at least similar to that of traditional liquid electrolytes.

Generation 5 cells includes Lithium-Sulphur (Li-S) batteries, which have already achieved 200 Wh/kg in current industrial prototypes [15]. Unfortunately, even though sulfur has a high specific capacity (1672 mAh/g) [15], sulfur active material dissolves during cycling, resulting in rapid capacity fading (i.e., shuttle effect) [16].

C. STATE OF THE ART AND CONTRIBUTION OF THE PRESENT STUDY

In the literature, several conventional LCAs have been performed focused on EV batteries, some of them, i.e., [5], [9], [10], [12], [14], [17], [18], [19], [20], [21], [22], and [23], addressing the environmental impacts of next-generation cells.

In [12], the life cycle environmental impacts of a SiNWs battery pack are compared with those of a current Li-ion battery pack. Nonetheless, no industrial scale-up for the SiNWs battery is performed. The environmental impacts of two next-generation cells are compared with those of a current Li-ion cell in [9], where the dependence of energy consumption on production volume is taken into account. In [10], the environmental impacts of two next-generation battery packs (i.e., Silicon NanoTubes (SiNTs) and SiNWs batteries) are compared with those of a current Li-ion battery pack. Nevertheless, for both SiNTs and SiNWs batteries, no industrial scale up is performed.

In [14], LCA is used to compare the environmental impacts of manufacturing All-Solid-State (ASS) batteries with those of current Li-ion batteries. Nonetheless, it is not mentioned whether a scale-up is performed. In [18], the environmental impacts of an ASS battery are assessed and a scale-up is performed by means of a scenario analysis.

In [15], an LCA of a Li-S battery pack is conducted by mixing laboratory- and industrial-scale data. In [19], a cradle-to-gate LCA of a Li-S cell is performed and several scenarios are presented for energy consumption reduction during cell production, cathode chemical composition, renewables uptake, and Li-S cell specific energy. In [20], the life cycle environmental impacts of a Li-S battery pack are compared with those of a current Li-ion battery pack. Nonetheless, no industrial scale up is performed. In [21], a cradle-to-grave LCA of a Li-S battery pack is performed based on a coin Li-S cell. In [17] and [22], the life cycle environmental impacts of Li-S battery packs are compared with those of current Li-ion battery packs without performing a scale-up. In [23], SSBs and Li-S batteries suitable for application to an aircraft are compared through cradle-to-gate LCA.

The aim of this study is to perform a P-LCA to compare the environmental impacts of four electrochemical pouch-type cells against those of a current Li-ion cell. In [24], the term ''ex-ante LCA'' refers to a method for scaling up low Technology Readiness Level (TRL) technologies, while the term P-LCA is used to compare various novel and conventional technologies at a future point in time. In [25], the term P-LCA refers to an ex-ante LCA mode that involves comparing technologies in a future point in time. In [8], several publications were examined and the terms P-LCA, anticipatory and ex-ante LCA were investigated; as a result subtle but not consistent differences were found among them. In [4], the three terms are used as synonyms while attention is paid to the distinction between scaling up in terms of TRL and time. According to [3], anticipatory LCA refers to an approach that includes also multiple social perspectives while the term ex-ante LCA is not mentioned. Hereafter, ex-ante LCA and P-LCA will be considered as synonyms and the term P-LCA will be used.

According to [4], the field of P-LCAs accounted for only 44 case studies in 2020, and these do not include batteries but rather other topic areas (i.e., mainly nanomaterials and chemicals). More recently, P-LCA has been applied to new bio-based polymers in [24], supercapacitors in [25], a novel froth flotation technology in [26] and wood-based technologies in [27]. To the best of our knowledge, only two P-LCA studies have been conducted in the battery field in [5] and [6] to estimate the environmental impacts of an ASS battery and a Li-S battery, respectively. However, a comparative P-LCA

TABLE 1. Product systems under study.

Product systems		Main parameters*		
		Specific capacity [Ah/kg]	Open circuit voltage [V]	Specific energy [Wh/kg]
Current Li-ion	Cathode: NMC622; Electrolyte: LiPF6 (liquid), EC, DMC; Anode: Graphite	55	3,8	209
SiNWs	Cathode: NMC622; Electrolyte: LiPF6 (liquid); Anode: SiNWs.	102,6	3,65	374
SiCPAN	Cathode: NMC622; Electrolyte: LiPF6 (liquid); Anode: SiCPAN.	97,4	3,8	370
ASS	Cathode: NMC622 with a Li2O–ZrO2 (LZO) coating.; Electrolyte: Li6PS5Cl (solid sulphide); Anode-free. The lithium deposition is enhanced by using an Ag-C nanocomposite layer on the stainless stell collector.	105,3	3,8	400
Li-S	Cathode: graphene-sulphur composite (GSC); Electrolyte: LiTFSi (liquid); Anode: Lithium metal	160,0	2,2	352

*Values are related to the worst-case scenario.

comprehensive of several next-generation cells for EV applications does not exist currently.

II. MATERIALS AND METHODS

This study was conducted in conformity with the most used frameworks for conventional LCAs, namely ISO 14040:2006 and ISO 14044:2018 [28], [29]. In addition, because the ISO standards do not provide guidance on how to conduct P-LCAs, the methodology was based on recent guidance that can be found in the literature [4], [7], [8], [30]. According to [24], the scaling up of life cycle inventories is accomplished through several techniques in the literature among which process-based simulations or calculation by means of projecting equations, definition of scenarios or scenario ranges. In this study, projecting equations and scenarios are used. Specifically, scenarios were set based on the guidelines reported in [4], [7], and [8] while projecting equations are from [21].

Hereafter, the assumptions made that can be shared with conventional LCAs (section A) and those related to P-LCAs are presented (section B).

A. CONVENTIONAL LCA

Herein the main items of the scope of the study are schematically described.

1) PRODUCT SYSTEM AND FUNCTIONAL UNIT

As reported in Table 1, the product systems under study are four novel electrochemical pouch-type cells: one SiCPAN, one SiNWs, one ASS, and one Li-S cell. The selection of the cells was driven by consultation with electrochemical and EV experts and literature. The main factors that have dictated this choice were:

- intention to include at least one cell from each of generations 3, 4, and 5.
- suitability for EVs.
- availability of data necessary to develop the study.

Current EVs use Li-ion batteries that allow for an average driving distance ranging between 250 and 400 km by recharging, while internal combustion engines allow for 1000 km driving distance by refueling [22]. According to [22], batteries should reach a specific energy of 550 Wh/kg in order to ensure a driving range of 500 km.

Silicon is one of the most promising anode materials for the next-generation EV batteries [31], [32]. It can store ten times more energy than graphite alone [33]. The higher energy density increases battery range while nanowires shorten charging time, both key metrics in EV uptake and acceptance [34]. Silicon is abundant enabling batteries with lower carbon footprint [35] and it is already being used in small amounts in the batteries of a few EV models, including Tesla Y, Tesla 3, and Porsche Taycan [36]. Two different silicon anode cells were chosen in this study: nanostructured (SiNWs) and micro-structured silicon anode cells (SiCPAN). Silicon below 150 nm has been found to be beneficial for solving silicon volume expansion [37]. Nevertheless, despite nanostructured silicon particles in conventional graphite electrodes have been implemented to commercial practice, this process is limited to the inclusion of only about 5% (by mass) of nano-silicon active material [13]. Also, nanoscale manufacturing is usually energy intensive and produces large amounts of nanowaste [12]. Instead, by encapsulating microstructured silicon particles in a PAN coating matrix, it seems possible to avoid both nanoscale manufacturing and silicon volume expansion. The method has been demonstrated in [13] at laboratory scale.

SSBs are promising technologies for the automotive sector for both their high energy density and safety [38]. ASS batteries are planned to be mass-produced by Samsung by 2027 for both EVs and consumer electronics [39]. Also, Nissan announced pilot-production by 2024 [40] while Volkswagen is in partnership with QuantumScape for enhancing development and mass-production of SSBs [41].

Li-S batteries are emerging as promising battery technology for EVs because they have high theoretical capacity and energy density without containing rare earth metals [5], [22].

As a result, the four cells in Table 1 were chosen as representatives of the main technologies currently being

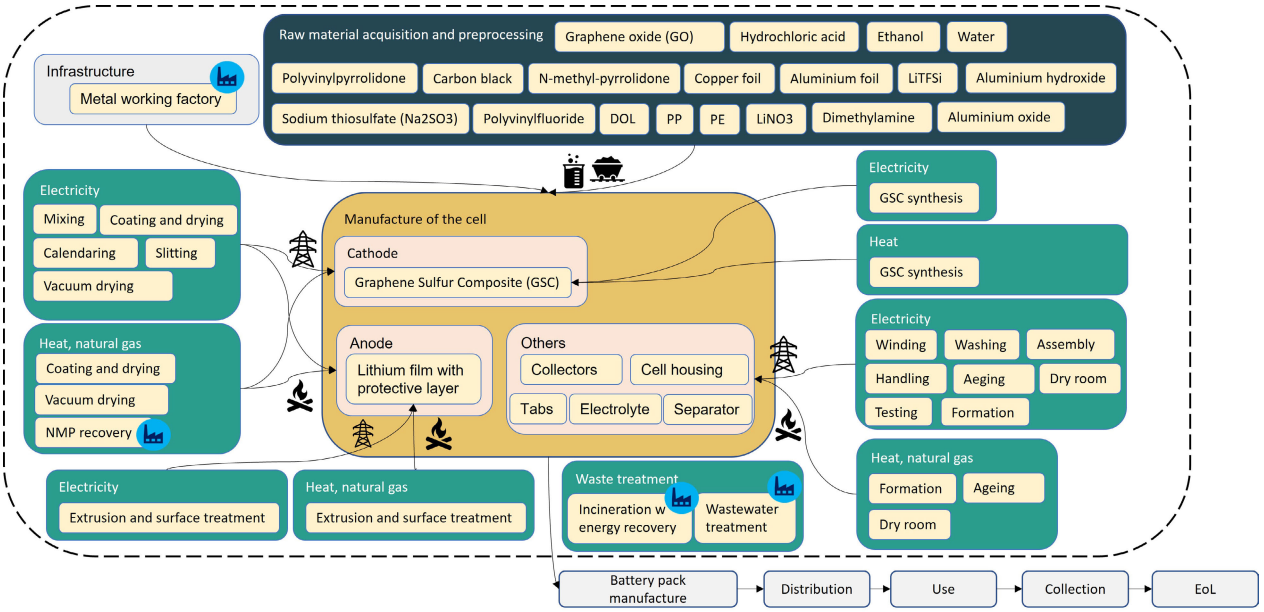

FIGURE 1. System boundary of the Li-S cell.

researched. The set of cells is compared to one Li-ion pouch-type cell, used as a benchmark for the analysis. To effectively compare the product systems under study, which differ significantly in terms of specific energy (kWh/kg), the functional unit is 1 kWh of rated energy capacity. The rated energy capacity is considered at cell level and thus, not impaired by the presence of the auxiliary battery components (i.e., BMS, cooling system and battery casing). The results of this article can be extended to battery pack level once the battery pack configuration is chosen.

2) SYSTEM BOUNDARY AND LIFE CYCLE IMPACT ASSESSMENT METHOD

The system boundary is cradle-to-gate. The analysis of the environmental impacts includes the extraction of raw materials for cell manufacturing, continues with the production of cell components and ends at the factory gate where the cells are assembled and finished. The use phase and the EoL phase were excluded from the system boundary because they are characterized by high uncertainty and lack of data [4], [6], especially when emerging technologies are considered.

Figure 1 takes as reference the Li-S cell to show the system boundary of this study. To highlight the differences between the laboratory- and industrial-scale boundaries, certain unit processes (e.g., infrastructure, solvent recovery, and waste treatment) are labelled with the blue icon of a plant. These unit processes are to be considered inside the boundary only in the case of industrial-scale production. For the Life Cycle Impact Assessment (LCIA), the most updated version of the Environmental Footprint (EF) method was used, in line with [42]. Background datasets were taken from Ecoinvent version 3.8 and SimaPro 9.3.0.3 was used as LCA software.

B. PROSPECTIVE LCA

According to [4], the following three challenges must be overcome when developing a P-LCA: data quality, comparability, and uncertainty. The following section explains how these three challenges have been addressed in this study. With reference to data quality, all data sources and the rationale for their selection are transparently reported (Section I, Figure 2). To address the issue of comparability, any laboratory scale data available for the next-generation cells was upscaled to industrial scale so that the time and the TRLs at which the comparison is made were aligned for all modelled technologies. The scaling procedure is shown in the flow scheme in Figure 4.

Lastly, to address uncertainty, two scenarios of future large-scale production were evaluated (Sections II-III) that combine different scenario parameters as shown in Table 2. The first scenario, called Worst Case Scenario (WCS), was developed to ensure comparability with current Li-ion cells, assuming that all the cells under study are mass produced in Europe today. Moreover, in the case of large uncertainties, the most pessimistic value of the uncertainty range was assumed in the WCS. The second scenario, called Best Case Scenario (BCS), intends to predict the sustainability performances of a future, greener, and more efficient production, if all the investigated cells, including the current Li-ion cell, are produced in Europe at a future point in time (i.e., 2040). Moreover, in the case of large uncertainties, the most optimistic value of the uncertainty range was assumed in the BCS. All the assumptions made in WCS and BCS are transparently reported (Sections II-III and Table 2). An extended scenario analysis considering three laboratory scale scenarios and five industrial scale scenarios was conducted for the Li-S cell and it is reported in the Appendix (Table 10s and Figure 1s).

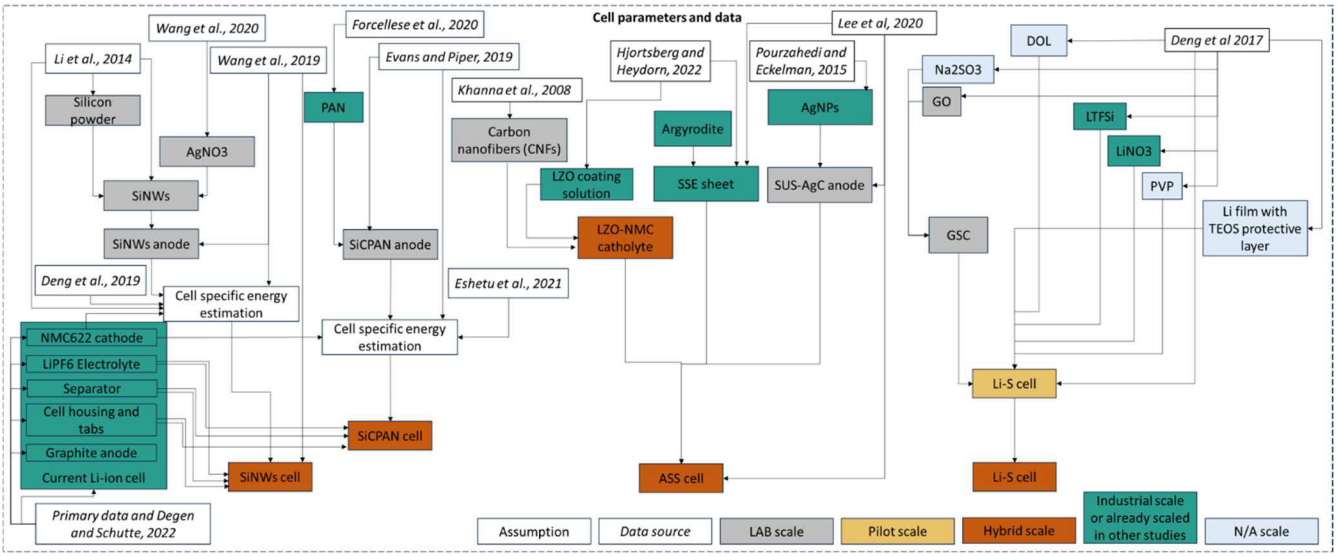

FIGURE 2. Overview of the data sources considered in this study.

TABLE 2. Scenario setting.

Scenario parameter		LAB	WCS	BCS
Specific energy (kWh/kg)	Current Li-ion	-	0,209	0,300
	SiNWs	0,374	0,374	0,400
	SiCPAN	0,370	0,370	0,400
	ASS	0,400	0,400	0,638
	Li-S	0,352	0,352	0,600
Solvent reduction		N	Y	Y
Solvent reduction rate (%)		-	20	20
Solvent recovery		N	Y	Y
Solvent recovery rate (%) *		-	68	80
Reuse of cleaning agents (one-time reuse) **		N	N	Y
Increased process yield ***		N	N	Y
Upscaling of waste treatment		N	Y	Y
2040 electricity mix		N	N	Y

*Except for HF and NMP.
**Only for the SiNWs cell.
***Only for silicon powder, SiNWs and VGCNF manufacturing processes.

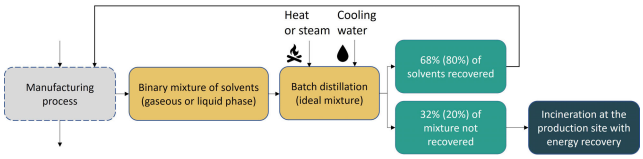

FIGURE 3. Solvent recovery model for the WCS. The recovery rates used for the BCS are reported within brackets.

1) DATA SOURCES FOR THE LABORATORY-SCALE INVENTORIES

Because next generation cells are currently characterized by a low TRL, P-LCA can be used in these cases to forecast the environmental impacts of emerging technologies starting from laboratory-scale data, usually taken from scientific articles, patents, expert interviews, unpublished results, and process simulations [4] and shifting them at a future point in time [5]. For the laboratory-scale cells, the data used in this study were collected from scientific literature, patents, and industry reports. Special attention was given to data source selection so that solely the publications in which data were presented in sufficient detail to be disaggregated, complemented and/or adjusted for the purpose of this study were selected. All data sources are shown in Figure 2.

The laboratory scale SiNWs cell design as well as the manufacturing of the SiNWs anode were based on the activity data of [10]. SiNWs were assumed to be produced through Metal-Assisted Chemical Etching (MACE), as described in [10] and [12]. According to [43] and [44], the MACE process is a widely used method to produce SiNWs. Hydrogen peroxide as oxidizing agent, silver nitrate as catalyst, and hydrogen fluoride as etching agent are used during the MACE process in compliance with [10] and [12].

The laboratory scale SiCPAN cell is comprised of a SiCPAN anode but the same cathode and electrolyte of the current Li-ion cell. The instructions reported in [13] were

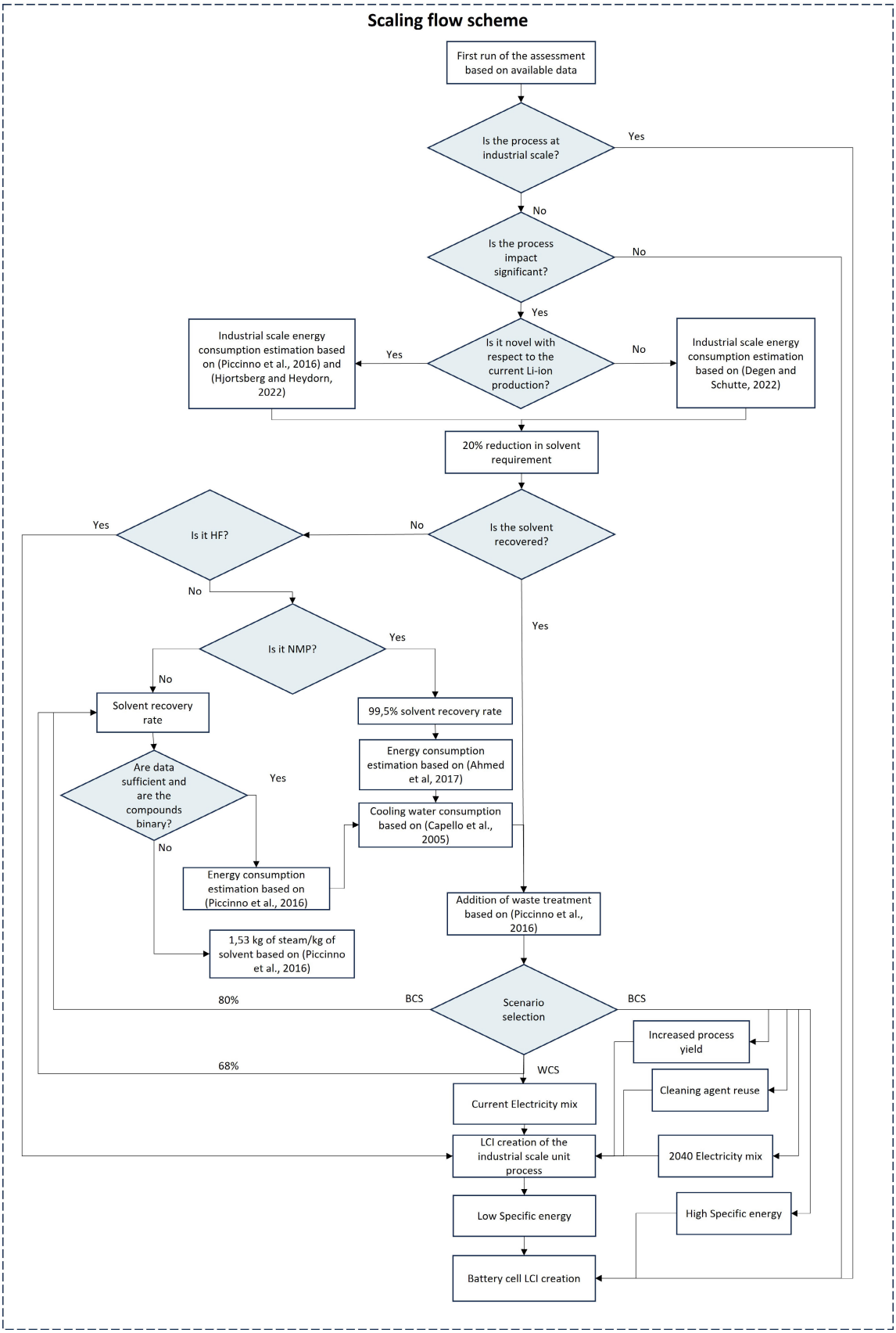

FIGURE 4. Scaling flow scheme.

used to model the SiCPAN anode assuming a 30% content of silicon. The process for PAN manufacturing was modelled as a polymerization of acrylonitrile according to [45]. The laboratory scale ASS cell was modelled based on [6], [46], [47], [48], [49], and [50]. The Vapor-Grown Carbon Nanofibers (VGCNFs) contained in the ASS cathode were assumed to be produced by catalytic pyrolysis as described in [47] and assuming benzene as carbon feedstock. According to [51], catalytic pyrolysis is currently the conventional and commercial technique for carbon nanofiber production. The synthesis process of the electrolyte (i.e., argyrodite) is based on [6] and [48]. The silver nanoparticles in the ASS anode were assumed to be synthesized by argon- and nitrogen-based Reactive Magnetron Sputtering (RMS) process as described in [49] and [50].

The laboratory scale Li-S cell is modelled based on [15], where laboratory-scale (i.e., data regarding the synthesis of graphene-sulfur cathode) and pilot-scale data (i.e., data regarding cell manufacturing) are mixed.

Lastly, for the current Li-ion cell, which is mass produced today and no scale up is needed, the raw material acquisition phase was based on primary data while the manufacturing plant data were taken from [52].

2) WORST CASE SCENARIO (WCS)

The WCS combines assumptions on the following three aspects of the production process: cell specific energy, energy consumption estimation during manufacturing, solvent reduction and recovery, and upscaling of waste treatment. All the scenario parameters and the assumptions made in the WCS are summarized in Table 2.

With reference to energy consumption, the energy flows of all the production steps that are equivalent or similar to those of the current Li-ion cell were modelled based on [52]. More specifically, for the coating and drying operations, electricity consumptions measured in kWh/kWh of cell capacity from [52] have been scaled proportionally to each cell capacity. Instead, the scale-up framework published in [30] was used for processes that differs from those involved in current Li-ion cell production (Figure 4).

With reference to solvent reduction and recovery, because the amount of each solvent used at the laboratory scale is higher than on the industrial scale, a 20% solvent reduction rate due to the scale-up was assumed in line with [30], and kept constant for both WCS and BCS scenarios. Also, a solvent recovery process was added (Figure 4). As a result, additional amounts of energy consumption and cooling water and certain solvent recovery rates were considered depending on the solvent type and scenario.

Because additional energy is needed for the recovery process, 6,09 kWh/kg_{NMP} of heat and 2,045 kWh/kg_{NMP} of electricity were added as energy inputs for the N-Methyl-Pyrrolidone (NMP) recovery in line with [53]. For the other solvents, conventional fractional distillation was assumed as the recovery process, and [30] was mainly used for the modelling of the process. Lastly, when [30] was not applicable (i.e., when data about properties or quantities of solvent were not sufficient, and in the case of non-binary compounds), 1,53 kg of steam per kg of solvent was assumed as proxy in compliance with [54]. Lastly, the recovery of hydrogen fluoride (i.e., the solvent used in the manufacturing of SiNWs) was not considered due to the high toxicity and ability of the HF to attach to particles in the air [10]. For this reason, it was assumed to be treated through incineration of hazardous waste.

For the cooling water, an average of 0,027 m^3 per kg of waste solvent was introduced for the condensation of the evaporated distillate, which has been empirically determined in [30].

The solvent recovery rate varies with scenarios, increasing from WCS to BCS. Regarding the WCS, in compliance with [30], a 68% solvent recovery rate is assumed for all the solvents, with the exception of NMP, for which a 99,5% recovery rate is assumed. This assumption is consistent with [53], [55] in which 99% and 99,5% NMP recovery rates are achieved, respectively.

With reference to waste treatment, incinerating spent solvents is the most common approach in the case of laboratory-scale productions [30] which leads to overestimated environmental impacts if assumed for industrial-scale. The up scaling of the waste treatment was performed based on [30]. Solvent that was not recovered was assumed to be treated at the production site through incineration with energy recovery, i.e., exploiting the enthalpy of solvent combustion to generate heat. Water that was not recovered was assumed to be processed through wastewater treatment. Lastly, all the spent substances that do not contain solvents were treated through hazardous waste incineration.

3) BEST CASE SCENARIO (BCS)

The BCS is meant to be a representation of an optimized industrial-scale scenario that combines assumptions on cell specific energy, solvent recovery, process yields, reuse of cleaning agents, and electricity mix decarbonization.

With respect to the BCS, the specific energies were increased based on what is expected in future or considering already achieved optimistic values (Table 1s and Table 2s).

For solvent recovery, the recovery rate was increased from 68% in the WCS to 80% in the BCS to use a comparable value with the NMP recovery rate achieved in the production of the current Li-ion cells, which ranges between 90 and 99,5% [53], [55] (Table 2).

Because yields are optimized in industrial-scale processes and the extent of variation between laboratory- and industrial-scale processes can vary by orders of magnitude [56], certain process yields were increased in the BCS to estimate economies of scale. For the SiNWs cell, because the laboratory-scale manufacturing process of silicon powder in [12] has a 75% yield, the industrial-scale manufacturing process of silicon powder was modelled as a grinding process

with 75% yield in the WCS and 95% yield in the BCS. The industrial-scale manufacturing process of SiNWs was modelled with 20% yield in the WCS and 40% yield in the BCS. For the ASS cell, to estimate economies of scale, the yield of the pyrolysis process used to produce VGCNFs was increased from 30% in the WCS to 50% in the BCS (Table 2).

To reduce the impact of the intensive use of cleaning agents in laboratory-scale processes, according to what is done for silicon wafers in [10], the amount of cleaning agents (i.e., acetone, ethanol, deionized water) used for SiNWs manufacturing was halved assuming a one-time reuse. Similarly, the amount of hydrochloric acid used for the purification of VGCNFs was halved (Table 2).

Lastly, in the BCS, the shift in terms of time scaling was accounted for by using for the whole foreground system the European electricity mix expected by 2040 in [57]. All the scenario parameters and the assumptions made in the BCS are summarized in Table 2.

III. RESULTS

The following midpoint Impact Categories (ICs) of the EF method were found to be the most relevant ones: climate change, acidification, eutrophication freshwater, ecotoxicity freshwater, resource use fossils and resource use of minerals and metals.

Hereafter, sections A, B and C are focused on the six most relevant ICs. SectionA refers to the comparison between laboratory- and industrial-scale environmental footprints of the Li-S cell (Figure 5), Section B refers to the comparison of all the product systems under study (Figure 6), and Section C refers to the hotspot analysis. Lastly, Section D refers to the comparison of all the product systems under study, considering all the ICs of the EF method (Figure 7-8). All the results are reported in Appendix.

In Figure 5-6, the environmental footprints are shown, separating the contributions of the cathode (illustrated in yellow), anode (light green), and other components (dark green). The cathode and anode contributions include the raw material extraction of active and inactive materials (i.e., additives, binders, and collectors) and energy consumption associated with the manufacturing of each electrode. All the other material and energy inputs are grouped under the category ''Others''.

A. EFFECT OF THE SCALING UP ON THE ENVIRONMENTAL FOOTPRINT OF THE LITHIUM-SULPHUR CELL

First, the laboratory scale and industrial scale environmental footprints of the Li-S cell were compared to investigate the potential environmental benefit due to the up-scaling (Figure 5).

Considering the WCS, climate change is reduced by 38% in the industrial scale production mainly because of the cathode (-20%) and other components (-18%). In terms of scenario settings, the significant reduction in the cathode contribution is mainly due to solvent reduction and recovery during GSC synthesis, which means partly avoiding the impacts of solvent production and incineration. The significant reduction in the other components contribution is mainly due to the scaling-up of energy consumption during cell manufacturing. The reduction between BCS and WCS mainly depends on the increase of the specific energy and adoption of the 2040 electricity mix.

The category related to the use of mineral and metal resources is not significantly affected by the scale-up from laboratory- to WCS industrial-scale, accounting for a 4% reduction only. In fact, in terms of scenario settings, the metal consumption is not directly affected by either energy consumption reduction, solvent reduction and recovery (i.e., solvents are water, ethanol, hydrogen peroxide and sulfuric acid) or up scaling of waste treatments. The significant reduction between WCS and BCS, is exclusively due to the higher specific energy of the cell in the BCS.

The other environmental impacts illustrated in Figure 5 are affected by reductions ranging from 23% to 51% passing from LAB to WCS and from 27% to 32% passing from WCS to BCS. The reductions from LAB to WCS in acidification, freshwater eutrophication, freshwater ecotoxicity and use of fossil resources are mainly driven by the up scaling of both the GSC synthesis and energy consumption during cell manufacturing. The reductions between BCS and WCS are significantly affected by the specific energy increase and adoption of the 2040 electricity mix in acidification, freshwater eutrophication, and use of fossil resources.

B. COMPARISON OF THE CELLS FOR THE SIX MOST RELEVANT IMPACT CATEGORIES IN THE BCS

Figure 6 shows the comparison of the environmental impacts of all the product systems under study for the six most relevant impact categories and considering the BCS. Similar results for the WCS can be found in the Appendix (Figure 2s).

For climate change, the current Li-ion cell results as the least impactful cell, accounting for 30,9 kg CO_{2eq}/kWh, followed by the SiCPAN cell, accounting for 42,0 kg CO_{2eq}/kWh. Contrarily, the SiNWs cell is the most impactful cell, accounting for 151,1 kg CO_{2eq}/kWh (i.e., more than three times the impact of the current Li-ion cell). This is mainly due to the SiNWs anode (80,8%), more specifically to the SiNWs manufacturing, which accounts for 75,7% of the entire impact of the SiNWs cell. Even more specifically, the key drivers in terms of climate change in SiNWs manufacturing are the silver nitrate production (36,6%), the disposal of hazardous wastes (19,5%), and the hydrogen fluoride production (9,3%). Furthermore, comparing the anode contributions to climate change of all the cells under study, the SiNWs anode has the highest impact. The ASS cell accounts for 78,5 kg CO_{2eq}/kWh (i.e., more than twice the impact of the current Li-ion cell). On one side, compared to the current Li-ion cell, the ASS cell benefits from a reduced cathode impact. This is due to the higher specific energy of the ASS cell resulting in lower material input requirements per kWh. On the other side, compared to the current Li-ion cell, the ASS cell has a greater anode impact. In fact, nearly 58% of the entire

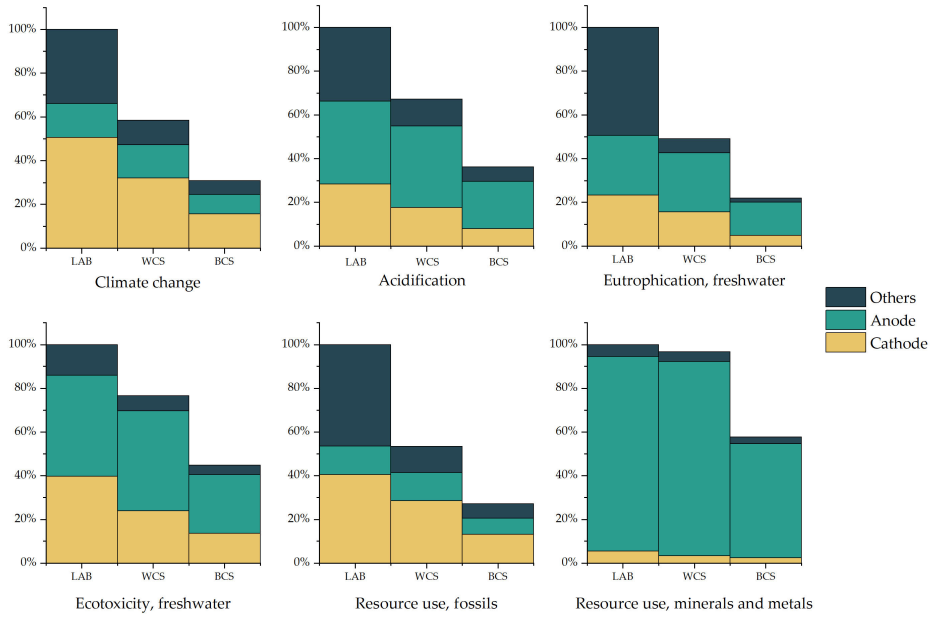

FIGURE 5. Comparison of the most relevant environmental impacts of laboratory and industrial scale productions of the Li-S cell. The impacts are normalized to the highest score in each category.

impact of the ASS cell is due to the anode, more specifically to the manufacturing of silver nanoparticles. Furthermore, the contribution of the ASS electrolyte is not significant in terms of climate change, accounting for only 5,7% of the entire impact of the ASS cell. Comparing all the electrolyte contributions to climate change, the ASS electrolyte stands at average between the most impactful (i.e., Li-S electrolyte) and the least impactful (i.e., SiCPAN and SiNWs electrolyte).

Lastly, the impact of the Li-S cell (52,9 kg CO_{2eq}/kWh) is almost twice the impact of the current Li-ion cell. This is mainly due to the impact of cathode production, mainly driven by the manufacturing of GSC (41,1%).

For acidification (Figure 6), the Li-S cell has the smallest impact, accounting for 0,36 mol $H+_{eq}$/kWh compared to the current Li-ion cell, accounting for 0,48 mol $H+_{eq}$/kWh. This is the result of the following two contributors: the Li-S anode, which is characterized by a significantly increased impact compared to the current Li-ion anode due to lithium production, and the GSC cathode, which is characterized by significantly reduced impact compared to the NMC cathode. Because different types of cathodes exist, the validity of the latter outcome is limited to the sulphur cathode considered in this study. With reference to the SiNWs cell, the anode continues to be the primary driver, accounting for 80,8% of the entire impact of the cell, making it the most impactful in terms of acidification.

For eutrophication of freshwater (Figure 6), all the cells are characterized by significantly higher impacts than the current Li-ion cell (0,025 kg P_{eq}/kWh). The Li-S cell accounts for 0,024 kg P_{eq}/kWh, the SiCPAN for 0,039 kg P_{eq}/kWh, the ASS cell for 0,138 kg P_{eq}/kWh and the SiNWs cell 0,206 kg P_{eq}/kWh. This is mainly due to the anodes of the cells, accounting for higher eutrophication impacts than the graphite anode. In the ASS cell, this is mainly due to silver nanoparticles production, accounting for 85% of the entire impact of the cell. The SiNWs cell remains the most impactful cell even in terms of eutrophication, where up to 92% of the entire impact is due to the manufacturing of SiNWs.

For ecotoxicity of freshwater (Figure 6), all the cells are characterized by higher impacts than the current Li-ion cell (2582 CTU_e/kWh). In fact, while the SiCPAN cathode has a comparable impact in terms of CTU_e/kWh as the NMC cathode, the SiCPAN anode is characterized by significantly higher impact than the graphite anode of the current Li-ion cell. Both the SiNWs and the ASS cells are characterized by even higher impacts than the current Li-ion cell. In fact, while the ASS and the SiNWs cathodes generate smaller impacts than the NMC cathode due to their higher specific energy, which results in lower material input requirements per kWh, the ASS and SiNWs anodes generate higher impacts than the graphite anode of the current Li-ion cell, due to the production of silver nitrate and silver nanoparticles, respectively.

For use of fossil resources (Figure 6), the SiCPAN and the current Li-ion cells are the least impactful cells accounting for 646 MJ/kWh and 531 MJ/kWh, respectively. The SiNWs, ASS and Li-S cells result in significantly higher impacts with respect to the current Li-ion cell.

For use of mineral and metal resources (Figure 6), the Li-S cell has the smallest impact. This is due to both the cathode, because the conventional NMC cathode is substituted with a sulphur cathode, and the anode, which accounts for a significantly lower impact with respect to the graphite

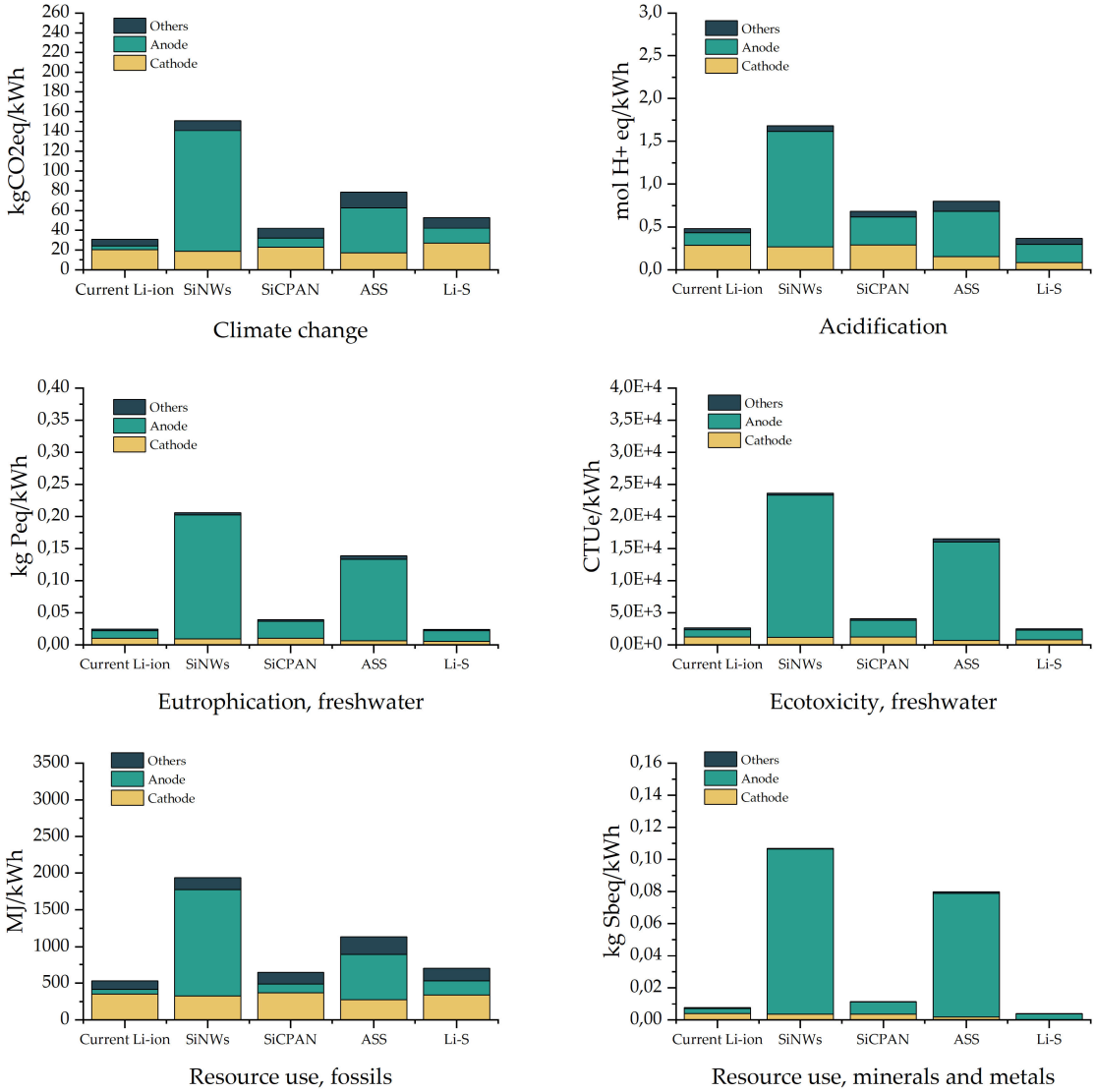

FIGURE 6. Comparison of the most relevant environmental impacts of the product systems under study divided by the functional unit (Combined BCS).

anode of the current Li-ion cell. Thus, the Li-S cell results are significantly less impactful (i.e., -47%) with respect to the current Li-ion cell. Contrarily, the SiNWs and ASS cells show significantly larger impacts than the current Li-ion cell, accounting for 0,107 and 0,080 $kgSb_{eq}$/kWh, respectively. This is due to the use of silver during the manufacturing of the two anodes. In fact, silver nitrate and silver nanoparticles account for 36,6% and 91,6% of the entire impacts of the SiNWs and ASS cells, respectively. Regarding the cathode of the ASS cell, although it is of the NMC-type (i.e., LZO-NMC) as the cathode of the current Li-ion cell, the lower impact with respect to the current Li-ion cell is due to the greater specific energy of the ASS cell, which results in lower material input requirements per kWh. Lastly, the SiCPAN cell is characterized by a higher impact (i.e., +53%) compared to the current Li-ion cell.

C. HOTSPOT ANALYSIS

This subsection aims to shed light on the main environmental hotspots of the product systems under study. For each cell and for each of the six most relevant impact categories, the main contributors of the impact are identified, and the most significant outcomes are reported.

The production of SiNWs is the key driver of the overall impact of the SiNWs cell, constituting the most impactful contributor in almost all the six most relevant ICs (i.e., ranging from a minimum of 74,8% in use of fossil resources up to 96,3% in use of mineral and metal resources). Within the production of the SiNWs three main hotspots are observed: the production of silver nitrate used as catalyst for the SiNWs process, the disposal of waste, and the production of hydrogen fluoride, especially in relation to the acidification.

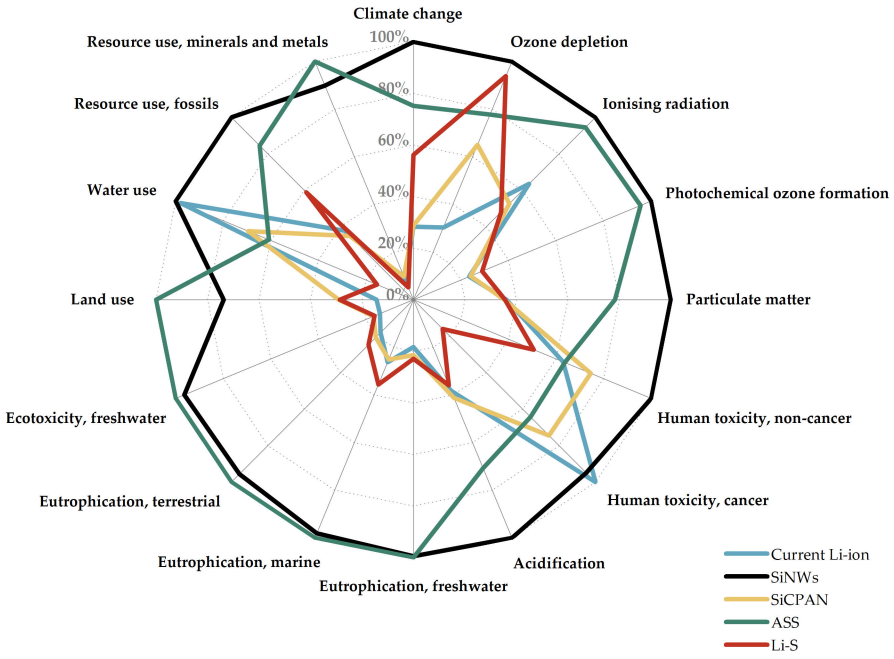

FIGURE 7. Comparison of the environmental impacts of the product systems under study considering all the 16 ICs of EF method and the WCS. The impacts are normalized to the highest score in each category.

For SiCPAN, in all the most relevant ICs, the two main contributors of the impacts are the active cathode materials and the copper current collector. It is worth noting that the production of the silicon powder and PAN have negligible influences on the impacts.

For the ASS cell, in all the most relevant ICs, the main contributor of the impact is the anode. More specifically, the production of silver nanoparticles generates the largest contribution ranging from 51% up to 97% of the cell impact. Such important contribution is associated to a small amount of material (i.e., 0,062 kg of silver nanoparticles per kWh of rated energy capacity). The active cathode material and the CNFs constitute the second and the third main contributors, respectively. The environmental footprint of the Li-S cell is mainly driven by the production of the GSC, lithium and copper in the current collector.

Nevertheless, except for climate change and use of fossil resources, the GSC cathode is significantly less impactful than the NMC cathode. This is due to the absence of the nickel-manganese-cobalt active material.

D. COMPARISON OF THE CELLS FOR ALL THE IMPACT CATEGORIES IN THE WCS AND BCS

Figures 7-8 show the sustainability performances of all the cells investigated in the present study, considering all the 16 ICs comprised in the EF method, using the WCS and BCS, respectively. As shown in Figure 7, in the WCS, the SiNWs cell generates the largest impacts in almost all the ICs. The Li-S and SiCPAN cells have lower impacts than the current Li-ion cell in 6 out of 16 and in 5 out of 16 ICs, respectively. As shown in Figure 8, in the BCS, the SiNWs cell generates the largest impacts in all the ICs. The Li-S and SiCPAN cells have lower impacts than the current Li-ion cell in 7 out of 16 and in 2 out of 16 ICs, respectively.

IV. DISCUSSION

While the sustainability of current Li-ion cells is limited by the usage of impactful critical metals in the cathode and by low specific energy, the SiCPAN and Li-S cells may overcome those limits and have lower or at least comparable environmental impacts. This study revealed that cells devoid of precious and critical metals are fundamental for ensuring sustainability, at least from a resource depletion perspective. For example, the Li-S cell has a climate change result comparable to the current Li-ion cell with a significantly lower use of mineral and metal resources.

According to [5] the impacts of the Li-S cell can be further reduced depending on the specific energy and the type of electrolyte salt. Moreover, with reference to the current Li-ion cell, primary data were used in this study resulting in 50,8 kg CO_{2eq}/kWh in the WCS and 30,9 kg CO_{2eq}/kWh in the BCS. Nevertheless, literature studies are characterized by a wide range of results in terms of climate change. Although Northvolt announced an NMC111 prismatic cell of 33 kg CO_{2eq}/kWh (2022 status) and expects to reach 10 kg CO_{2eq}/kWh by 2030 [58], it must be pointed out that an NMC cell can reach up to 100 kg CO_{2eq}/kWh [58], [59].

Because the next-generation cells have climate change results ranging from 42 to 151 kg CO_{2eq}/kWh in the BCS, improvements in terms of sustainability are needed. For

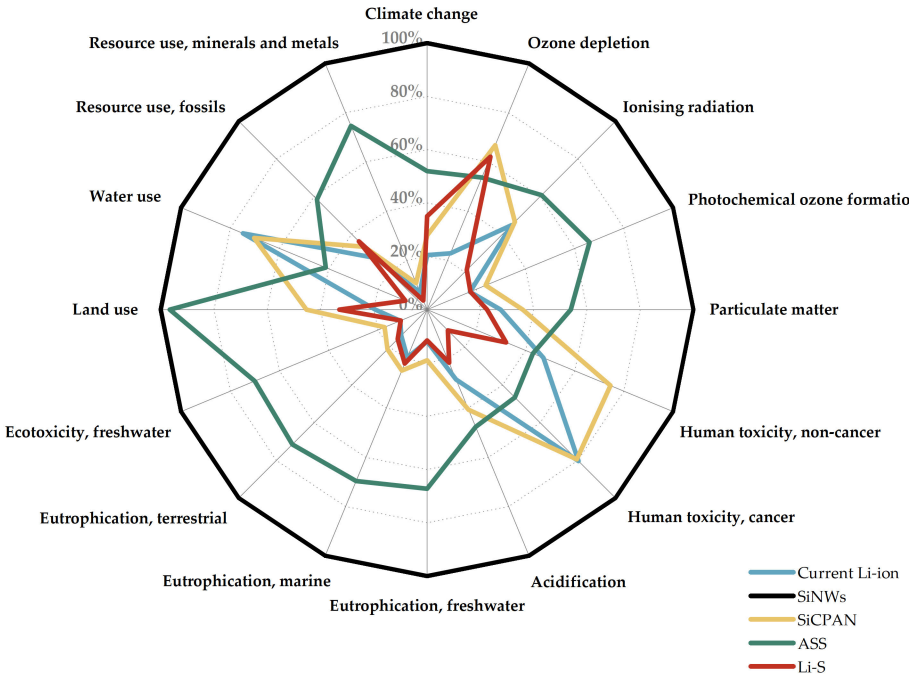

FIGURE 8. Comparison of the environmental impacts of the product systems under study considering all the 16 ICs of EF method and the BCS. The impacts are normalized to the highest score in each category.

example, the SiNWs cell resulted in the greatest impacts primarily due to silver nitrate used as catalyst for SiNWs manufacturing. For a transition to green SSBs, the adoption of other cell chemical compositions, such as without protective layers containing silver nanoparticles, may significantly change the results obtained in this study. The results of a what-if analysis assuming that silver is not used in both the SiNWs and ASS cells revealed that the ASS cell produced without silver nanoparticles would be the least impactful cell among the next-generation cells considered in this study (Figure 3s).

Lastly, it must be pointed out that this study has a cradle-to-gate boundary. In fact, use and end-of-life phases were neglected because of lack of data regarding the durability and the recycling and disposal processes of the next generation cells. The adoption of a cradle-to-grave boundary may significantly change the results of this study depending on the assumed cycle life and recycling process.

Lastly, only primary materials were used as input in this investigation. However, secondary materials from scrap can be used to produce battery cells in the future. For instance, the usage of secondary silver might significantly alter the outcome. Nevertheless, because secondary materials require some treatments, before their reuse, this may compromise the environmental advantages of secondary materials over primary materials [60]. For this reason, the use of secondary materials will be addressed in a dedicated work.

Potential limitations regarding the assumptions made in this study are reported in the Appendix (Section A.8).

V. CONCLUSION

Prospective LCAs can be useful tools for making environmental sustainability a design criterion already at the early stages of the battery production process. In this study, a cradle-to-gate P-LCA was performed to compare the environmental impacts of a current Li-ion cell used as a benchmark and a set of next-generation cells suitable for EV application: two silicon-anode cells (i.e., SiNWs and SiCPAN), a solid-state cell (i.e., ASS) and a Lithium-Sulphur cell (i.e., Li-S). To effectively compare the environmental sustainability of the cells, laboratory-scale data of the next-generation cells were up scaled. Lastly, two scenarios were considered, namely the WCS and the BCS.

First, the effects of upscaling the manufacturing was presented for the Li-S cell for both the WCS and the BCS. It was observed that the scale-up has a meaningful effect on the climate change impact, which is reduced by roughly 40% in the WCS.

Second, the product systems were compared considering the six most relevant impact categories. Assuming the BCS, in four out of six ICs, the Li-S cell resulted to have lower impact with respect to the current Li-ion cell. In particular, it exhibited reduced resource use of minerals and metals compared to the current Li-ion cell because of the absence of the NMC cathode and precious metals in the manufacturing process. The impacts of the Li-S cell may be further reduced depending on the specific energy and the type of electrolyte salt.

The ASS cell had significant higher impacts than the current Li-ion cell in all the impact categories assuming the BCS, owing to silver nanoparticles. The SiNWs cell had the greatest impacts in all the six ICs because of the SiNWs production. According to the hotspot analysis, either for the SiNWs or ASS cells, the silver usage is a key driver for the impacts, especially in terms of resource use of minerals and metals and ecotoxicity. The potential production of SiNWs and ASS cells without the use of silver would result in a drastic reduction of the environmental burdens. In particular, the ASS cell would become the least impacting cell among the next generation cells.

Lastly, considering the entire battery pack, a cradle-to-grave boundary and/or the use of recycled material may result in different or additional outcomes.

REFERENCES

[1] *Strategic Research Agenda for Batteries*, Batteries Europe, European Commission, Brussels, Belgium, 2020.

[2] T. Schmaltz, T. Wicke, L. Weymann, P. Voß, C. Neef, and A. Thielmann, "Solid-state battery roadmap 2035+," Fraunhofer Inst. Syst. Innov. Res., Germany, Version, Sep. 2022, doi: 10.24406/PUBLICA-68.

[3] J. B. Guinée, S. Cucurachi, P. J. G. Henriksson, and R. Heijungs, "Digesting the alphabet soup of LCA," *Int. J. Life Cycle Assessment*, vol. 23, no. 7, pp. 1507–1511, Jul. 2018, doi: 10.1007/s11367-018-1478-0.

[4] N. Thonemann, A. Schulte, and D. Maga, "How to conduct prospective life cycle assessment for emerging technologies? A systematic review and methodological guidance," *Sustainability*, vol. 12, no. 3, p. 1192, Feb. 2020, doi: 10.3390/su12031192.

[5] S. Wickerts, R. Arvidsson, A. Nordelöf, M. Svanström, and P. Johansson, "Prospective life cycle assessment of lithium-sulfur batteries for stationary energy storage," *ACS Sustain. Chem. Eng.*, vol. 11, no. 26, pp. 9553–9563, Jul. 2023, doi: 10.1021/acssuschemeng.3c00141.

[6] S. Hjortsberg and Z. Heydorn, "Prospective life-cycle assessment of an argyrodite type solid-state battery," M.S. thesis, Dept. Technol. Manag. Econ., Division Environ. Syst. Anal., Chalmers Univ. Technol., Gothenburg, Sweden, 2022.

[7] R. Arvidsson, A. Tillman, B. A. Sandén, M. Janssen, A. Nordelöf, D. Kushnir, and S. Molander, "Environmental assessment of emerging technologies: Recommendations for prospective LCA," *J. Ind. Ecol.*, vol. 22, no. 6, pp. 1286–1294, Dec. 2018, doi: 10.1111/jiec.12690.

[8] M. Buyle, A. Audenaert, P. Billen, K. Boonen, and S. Van Passel, "The future of ex-ante LCA? Lessons learned and practical recommendations," *Sustainability*, vol. 11, no. 19, p. 5456, Oct. 2019, doi: 10.3390/su11195456.

[9] W. Zheshan and K. Defei, "Comparative life cycle assessment of lithium-ion batteries with lithium metal, silicon nanowire, and graphite anodes," *Clean Technol. Environ. Policy*, vol. 20, pp. 1233–1244, May 2018, doi: 10.1007/s10098-018-1548-9.

[10] F. Wang, X. Gao, L. Ma, and C. Yuan, "Environmental sustainability of metal-assisted chemical etching of silicon nanowires for lithium-ion battery anode," *J. Electrochem. Energy Convers. Storage*, vol. 17, no. 1, Feb. 2020, Art. no. 011012, doi: 10.1115/1.4044957.

[11] B. M. Bang, H. Kim, H.-K. Song, J. Cho, and S. Park, "Scalable approach to multi-dimensional bulk Si anodes via metal-assisted chemical etching," *Energy Environ. Sci.*, vol. 4, no. 12, p. 5013, 2011, doi: 10.1039/c1ee02310a.

[12] B. Li, X. Gao, J. Li, and C. Yuan, "Life cycle environmental impact of high-capacity lithium ion battery with silicon nanowires anode for electric vehicles," *Environ. Sci. Technol.*, vol. 48, no. 5, pp. 3047–3055, Mar. 2014, doi: 10.1021/es4037786.

[13] T. Evans and D. M. Piper, "Large-format battery anodes comprising silicon particles," U.S. Patent Appl. 17/808 285.

[14] R. Pell, J. J. Lindsay, P. Whattoff, and L. Tijsseling, "Comparative life cycle assessment study of solid state and lithium-ion batteries for electric vehicle application in Europe," Minviro Ltd, U.K., Version 3.0, Tech. Rep., 2021, p. 77.

[15] Y. Deng, J. Li, T. Li, X. Gao, and C. Yuan, "Life cycle assessment of lithium sulfur battery for electric vehicles," *J. Power Sources*, vol. 343, pp. 284–295, Mar. 2017, doi: 10.1016/j.jpowsour.2017.01.036.

[16] B. Gong, X. Song, Y. Shi, J. Liu, and C. Hao, "Understanding the inhibition of the shuttle effect of sulfides ($S \leq 3$) in Lithium–Sulfur batteries by heteroatom-doped graphene: First-principles study," *J. Phys. Chem. C*, vol. 124, no. 6, pp. 3644–3649, Feb. 2020, doi: 10.1021/acs.jpcc.9b10314.

[17] S. Lopez, O. Akizu-Gardoki, and E. Lizundia, "Comparative life cycle assessment of high performance lithium-sulfur battery cathodes," *J. Cleaner Prod.*, vol. 282, Feb. 2021, Art. no. 124528, doi: 10.1016/j.jclepro.2020.124528.

[18] S. Troy, A. Schreiber, T. Reppert, H.-G. Gehrke, M. Finsterbusch, S. Uhlenbruck, and P. Stenzel, "Life cycle assessment and resource analysis of all-solid-state batteries," *Appl. Energy*, vol. 169, pp. 757–767, May 2016, doi: 10.1016/j.apenergy.2016.02.064.

[19] R. Arvidsson, M. Janssen, M. Svanström, P. Johansson, and B. A. Sandén, "Energy use and climate change improvements of Li/S batteries based on life cycle assessment," *J. Power Sources*, vol. 383, pp. 87–92, Apr. 2018, doi: 10.1016/j.jpowsour.2018.02.054.

[20] F. Cerdas, P. Titscher, N. Bognar, R. Schmuch, M. Winter, A. Kwade, and C. Herrmann, "Exploring the effect of increased energy density on the environmental impacts of traction batteries: A comparison of energy optimized lithium-ion and lithium-sulfur batteries for mobility applications," *Energies*, vol. 11, no. 1, p. 150, Jan. 2018, doi: 10.3390/en11010150.

[21] D. Wolff, L. C. Casals, G. Benveniste, C. Corchero, and L. Trilla, "The effects of lithium sulfur battery ageing on second-life possibilities and environmental life cycle assessment studies," *Energies*, vol. 12, no. 12, p. 2440, Jun. 2019, doi: 10.3390/en12122440.

[22] G. Benveniste, A. Sánchez, H. Rallo, C. Corchero, and B. Amante, "Comparative life cycle assessment of li-sulphur and Li-ion batteries for electric vehicles," *Resour., Conservation Recycling Adv.*, vol. 15, Nov. 2022, Art. no. 200086, doi: 10.1016/j.rcradv.2022.200086.

[23] A. Barke, W. Cistjakov, D. Steckermeier, C. Thies, J. Popien, P. Michalowski, S. P. Melo, F. Cerdas, C. Herrmann, U. Krewer, A. Kwade, and T. S. Spengler, "Green batteries for clean skies: Sustainability assessment of lithium-sulfur all-solid-state batteries for electric aircraft," *J. Ind. Ecol.*, vol. 27, no. 3, pp. 795–810, Jun. 2023, doi: 10.1111/jiec.13345.

[24] N. R. D. de Souza, L. Matt, R. Sedrik, L. Vares, and F. Cherubini, "Integrating ex-ante and prospective life-cycle assessment for advancing the environmental impact analysis of emerging bio-based technologies," *Sustain. Prod. Consumption*, vol. 43, pp. 319–332, Dec. 2023, doi: 10.1016/j.spc.2023.11.002.

[25] A. K. Kamali, E. Glogic, N. M. Keppetipola, G. Sonnemann, T. Toupance, and L. Cojocaru, "Prospective life cycle assessment of two supercapacitor architectures," *ACS Sustain. Chem. Eng.*, vol. 11, no. 44, pp. 15898–15909, Nov. 2023, doi: 10.1021/acssuschemeng.3c04007.

[26] H. Eltohamy, G. Cecere, and L. Rigamonti, "Ex-ante life cycle assessment of FineFuture flotation technology: Case study of Grecian Magnesite," *Int. J. Life Cycle Assessment*, vol. 28, no. 10, pp. 1348–1365, Oct. 2023, doi: 10.1007/s11367-023-02221-6.

[27] A. Sander-Titgemeyer, M. Risse, and G. Weber-Blaschke, "Applying an iterative prospective LCA approach to emerging wood-based technologies: Three German case studies," *Int. J. Life Cycle Assessment*, vol. 28, no. 5, pp. 495–515, May 2023, doi: 10.1007/s11367-023-02139-z.

[28] *Environmental Management. Life Cycle Assessment. Principles and Framework. Place of Publication Not Identified: Bsi*, document ISO, ISO 14040:2006, 2006.

[29] *Environmental management. Life cycle assessment. Requirements and guidelines, Withdrawn*, document ISO, ISO 14044:2006, 2018.

[30] F. Piccinno, R. Hischier, S. Seeger, and C. Som, "From laboratory to industrial scale: A scale-up framework for chemical processes in life cycle assessment studies," *J. Cleaner Prod.*, vol. 135, pp. 1085–1097, Nov. 2016, doi: 10.1016/j.jclepro.2016.06.164.

[31] X. Shen, Z. Tian, R. Fan, L. Shao, D. Zhang, G. Cao, L. Kou, and Y. Bai, "Research progress on silicon/carbon composite anode materials for lithium-ion battery," *J. Energy Chem.*, vol. 27, no. 4, pp. 1067–1090, Jul. 2018, doi: 10.1016/j.jechem.2017.12.012.

[32] F. Luo, B. Liu, J. Zheng, G. Chu, K. Zhong, H. Li, X. Huang, and L. Chen, "Review—nano-silicon/carbon composite anode materials towards practical application for next generation li-ion batteries," *J. Electrochem. Soc.*, vol. 162, no. 14, pp. A2509–A2528, Oct. 2015, doi: 10.1149/2.0131514jes.

[33] M. Ashuri, Q. He, and L. L. Shaw, "Silicon as a potential anode material for Li-ion batteries: Where size, geometry and structure matter," *Nanoscale*, vol. 8, no. 1, pp. 74–103, Dec. 2016, doi: 10.1039/c5nr05116a.

[34] M. Lampinen. *Silicon Nanowires A*. Accessed: Dec. 11, 2023. [Online]. Available: https://www.automotiveworld.com/articles/silicon-nanowires-a-breakthrough-for-electric-future-says-karl-thomas-neumann/

[35] P. Sehrawat, A. Shabir, Abid, C. M. Julien, and S. S. Islam, "Recent trends in silicon/graphene nanocomposite anodes for lithium-ion batteries," *J. Power Sources*, vol. 501, Jul. 2021, Art. no. 229709, doi: 10.1016/j.jpowsour.2021.229709.

[36] AZoCleantech.com. *Making Electric Vehicles More Sustainable With Silicon Nanowire Technology*. Accessed: Dec. 30, 2023. [Online]. Available: https://www.azocleantech.com/article.aspx?ArticleID=1366

[37] K. Nishikawa, J. Moon, and K. Kanamura, "In-situ observation of volume expansion behavior of a silicon particle in various electrolytes," *J. Power Sources*, vol. 302, pp. 46–52, Jan. 2016, doi: 10.1016/j.jpowsour.2015.10.014.

[38] M. B. Dixit, A. Parejiya, N. Muralidharan, R. Essehli, R. Amin, and I. Belharouak, "Understanding implications of cathode architecture on energy density of solid-state batteries," *Energy Storage Mater.*, vol. 40, pp. 239–249, Sep. 2021, doi: 10.1016/j.ensm.2021.05.001.

[39] O. Sohail. (2027). *Samsung Aims to Launch Solid-State Batteries By 2027, But Its Smartphones Will Not Be the First to Use Them*. Accessed: Dec. 30, 2023. [Online]. Available: https://wccftech.com/samsung-developing-solid-state-batteries-launch-in-2027/

[40] *All Solid-State Battery: Could Nissan Make It First? | Electrive.com*. Accessed: Dec. 30, 2023. [Online]. Available: https://www.electrive.com/2022/04/18/nissan-all-solid-state-battery-will-nissan-make-it-first/

[41] *Volkswagen Invests $200 Million in QuantumScape | Electrive.com*. Accessed: Dec. 30, 2023. [Online]. Available: https://www.electrive.com/2020/06/16/volkswagen-invests-200-million-in-quantumscape/

[42] S. Manfredi, K. Allacker, N. Pelletier, and D. M. de Souza, "Product environmental footprint (PEF) guide," Eur. Commission—Joint Res. Centre, Ispra, Italy, Tech. Rep., 2012.

[43] M. A. Alher, A. Mosleh, and S. F. Banihashemian, "Investigation of silicon nanowires produced by metal-assisted chemical etching method," *IOP Conf. Ser. Mater. Sci. Eng.*, vol. 671, no. 1, Art. no. 012028, Jan. 2020, doi: 10.1088/1757-899X/671/1/012028.

[44] A. A. Leonardi, M. J. L. Faro, and A. Irrera, "Silicon nanowires synthesis by metal-assisted chemical etching: A review," *Nanomaterials*, vol. 11, no. 2, p. 383, Feb. 2021, doi: 10.3390/nano11020383.

[45] A. Forcellese, M. Marconi, M. Simoncini, and A. Vita, "Life cycle impact assessment of different manufacturing technologies for automotive CFRP components," *J. Cleaner Prod.*, vol. 271, Oct. 2020, Art. no. 122677, doi: 10.1016/j.jclepro.2020.122677.

[46] Y.-G. Lee, S. Fujiki, C. Jung, N. Suzuki, N. Yashiro, R. Omoda, D.-S. Ko, T. Shiratsuchi, T. Sugimoto, S. Ryu, J. H. Ku, T. Watanabe, Y. Park, Y. Aihara, D. Im, and I. T. Han, "High-energy long-cycling all-solid-state lithium metal batteries enabled by silver–carbon composite anodes," *Nature Energy*, vol. 5, no. 4, pp. 299–308, Mar. 2020, doi: 10.1038/s41560-020-0575-z.

[47] V. Khanna, B. R. Bakshi, and L. J. Lee, "Carbon nanofiber production," *J. Ind. Ecol.*, vol. 12, no. 3, pp. 394–410, Jun. 2008, doi: 10.1111/j.1530-9290.2008.00052.x.

[48] L. Zhou, K.-H. Park, X. Sun, F. Lalère, T. Adermann, P. Hartmann, and L. F. Nazar, "Solvent-engineered design of argyrodite Li_6PS_5X (X = cl, br, I) solid electrolytes with high ionic conductivity," *ACS Energy Lett.*, vol. 4, no. 1, pp. 265–270, Jan. 2019, doi: 10.1021/acsenergylett.8b01997.

[49] L. Pourzahedi and M. J. Eckelman, "Comparative life cycle assessment of silver nanoparticle synthesis routes," *Environ. Sci., Nano*, vol. 2, no. 4, pp. 361–369, 2015, doi: 10.1039/c5en00075k.

[50] S. Temizel-Sekeryan and A. L. Hicks, "Global environmental impacts of silver nanoparticle production methods supported by life cycle assessment," *Resour., Conservation Recycling*, vol. 156, May 2020, Art. no. 104676, doi: 10.1016/j.resconrec.2019.104676.

[51] D. Yadav, F. Amini, and A. Ehrmann, "Recent advances in carbon nanofibers and their applications—A review," *Eur. Polym. J.*, vol. 138, Sep. 2020, Art. no. 109963, doi: 10.1016/j.eurpolymj.2020.109963.

[52] F. Degen and M. Schütte, "Life cycle assessment of the energy consumption and GHG emissions of state-of-the-art automotive battery cell production," *J. Cleaner Prod.*, vol. 330, Jan. 2022, Art. no. 129798, doi: 10.1016/j.jclepro.2021.129798.

[53] S. Ahmed, P. A. Nelson, K. G. Gallagher, and D. W. Dees, "Energy impact of cathode drying and solvent recovery during lithium-ion battery manufacturing," *J. Power Sources*, vol. 322, pp. 169–178, Aug. 2016, doi: 10.1016/j.jpowsour.2016.04.102.

[54] R. Hischier, S. Hellweg, C. Capello, and A. Primas, "Establishing life cycle inventories of chemicals based on differing data availability (9 pp)," *Int. J. Life Cycle Assessment*, vol. 10, no. 1, pp. 59–67, Jan. 2005, doi: 10.1065/lca2004.10.181.7.

[55] Q. Dai, J. Spangenberger, S. Ahmed, L. Gaines, J. C. Kelly, and M. Wang, *EverBatt: A Closed-Loop Battery Recycling Cost and Environmental Impacts Model*, document ANL-19/16, 1530874, Apr. 2019, doi: 10.2172/1530874.

[56] G. Pallas, M. G. Vijver, W. J. G. M. Peijnenburg, and J. Guinée, "Ex ante life cycle assessment of GaAs/Si nanowire–based tandem solar cells: A benchmark for industrialization," *Int. J. Life Cycle Assessment*, vol. 25, no. 9, pp. 1767–1782, Sep. 2020, doi: 10.1007/s11367-020-01791-z.

[57] *Net Zero by 2050, A Roadmap for the Global Energy Sector*, IEA, Paris, France, 2021.

[58] Northvolt. (2022). *Sustainability and Annual Report 2022*. Accessed: Jan. 11, 2024. [Online]. Available: https://www.datocms-assets.com/38709/1684304946-northvolt_sustainability_and_annual_report_2022.pdf

[59] M. Abdelbaky, L. Schwich, J. Henriques, B. Friedrich, J. R. Peeters, and W. Dewulf, "Global warming potential of lithium-ion battery cell production: Determining influential primary and secondary raw material supply routes," *Cleaner Logistics Supply Chain*, vol. 9, Dec. 2023, Art. no. 100130, doi: 10.1016/j.clscn.2023.100130.

[60] E. Bontempi, "How to perform a material recovery sustainability evaluation preliminary to LCA?" *Resour., Environ. Sustainability*, vol. 9, Sep. 2022, Art. no. 100074, doi: 10.1016/j.resenv.2022.100074.

ANTONELLA ACCARDO was born in Palermo, Italy, in 1993. She received the B.S. and M.S. degrees in mechanical engineering from Politecnico di Torino, Italy, in 2019, where she is currently pursuing the Ph.D. degree with the Department of Energy.

After graduating, she was a Research Fellow with the Department of Energy, Politecnico di Torino, for two years. She is a member of the Interdepartmental Center for Automotive Research and Sustainable Mobility (CARS), Politecnico di Torino. Her research interests include the sustainability of the transport sector, including the application of life cycle assessment and life cycle costing to light- and heavy-duty commercial vehicles and their main components, such as batteries, electric motors, hydrogen, and internal combustion engines and fuel cells.

AMBROGIO GAROFALO was born in Cosenza, Italy, in 1999. He received the B.S. degree in mechanical engineering and the M.S. degree in automotive engineering from Politecnico di Torino, in 2021 and 2022, respectively.

GIOVANNI DOTELLI received the M.S. degree in chemical engineering and the Ph.D. degree in materials engineering from Politecnico di Milano, Italy, in 1989 and 1993, respectively.

He is currently a Full Professor of materials science with the Dipartimento di Chimica, Materiali e Ingegneria Chimica "Giulio Natta," Politecnico di Milano, where he is in charge of the Laboratory of Materials for Energy and Environment. His current research interests include materials for energy- and environmental-related sustainable technologies.

EZIO SPESSA received the M.S. degree in mechanical engineering and the Ph.D. degree in energetics from Politecnico di Torino, Italy, in 1991 and 1995, respectively.

He is currently a Full Professor of fluid machinery with the Dipartimento Energia "Galileo Ferraris," Politecnico di Torino, and a member of the Interdepartmental Center for Automotive Research and Sustainable Mobility (CARS), Politecnico di Torino. His research interests include innovative vehicle technologies and powertrain solutions for the zero-tailpipe emission mobility of people and goods, including LCA approaches and circular economy aspects for sustainable and innovative road mobility solutions.